Two- and three-particle femtoscopy in small collision systems at LHCb

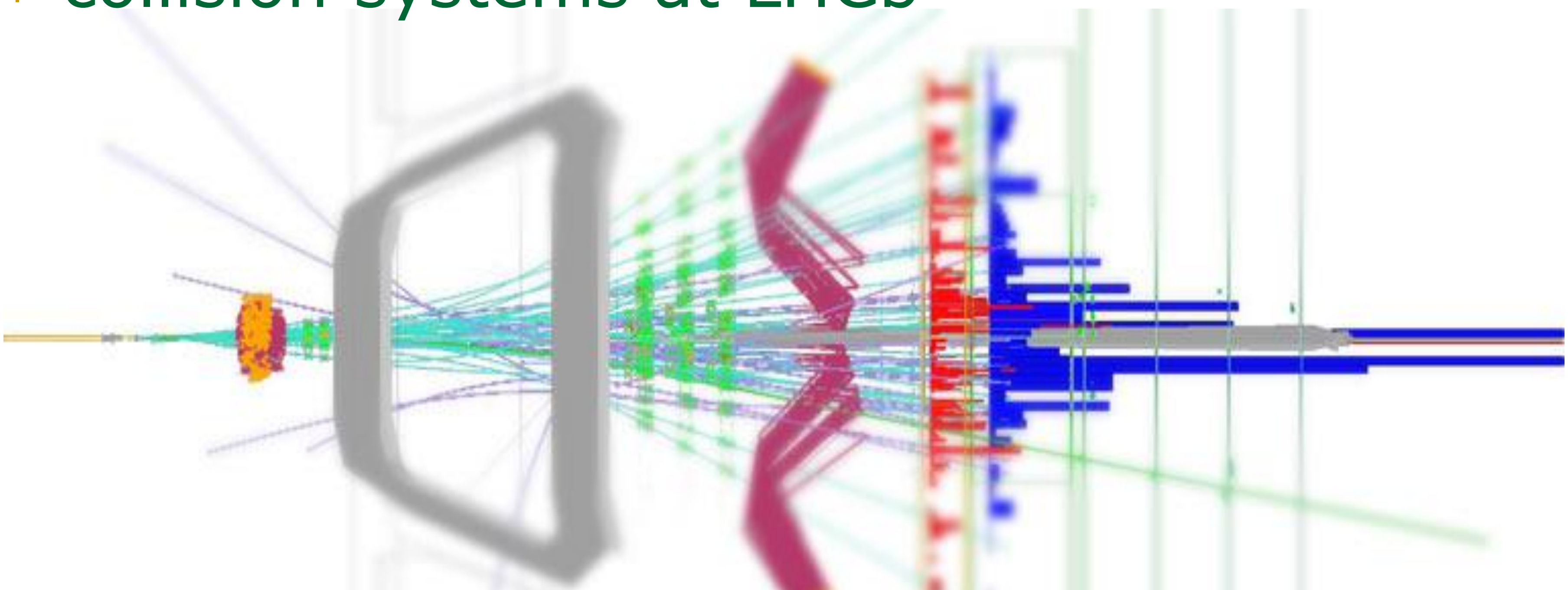

Marcin Kucharczyk

IFJ PAN, Kraków

Seminarium IFJ PAN
29 January 2026

Outline

- Quantum correlations in particle physics
- LHCb - general purpose forward experiment
- BEC for pion pairs in *pp* collisions at 7 TeV [JHEP 12 (2017) 025]
- BEC in *pPb* at 5 TeV [JHEP 09 (2023) 172]
- Three-pion BEC in *pp* collisions [JHEP 08 (2025) 174]
- Conclusions

Quantum correlations in particle physics

Historically (analogue to Hanbury-Brown-Twiss intensity interferometry)

- 1959: Goldhaber, Goldhaber, Lee and Pais
- experiment at the Bevalac/LBL in Berkeley
- looking at resonances by comparing *Q* distribution of unlike-sign pion pairs to like-sign
- unexpected angular correlation for like-sign pions

In particle physics:

- symmetrization *(Bose-Einstein Correlations - BEC)* and antisymmetrization *(Fermi-Dirac Correlations - FDC)* of total wave function
- correlations in four-momenta of indistinguishable particles emitted from same source:

$$Q = \sqrt{-(q_1 - q_2)^2} = \sqrt{M^2 - 4\mu^2}$$

- useful tool to probe spatial and temporal structure of hadron emission volume

Effect studied across many collision systems with wide spectrum of energies:

- many results on BEC/FDC from LEP
- also performed by ALICE, ATLAS, CMS and LHCb (LHC), STAR and PHENIX (RHIC), SPS,...

Motivation: 2-particle BEC

- Bose-Einstein Correlations
  - → useful to probe size of particle emission at kinetic freeze-out
  - → looking for collective effects in small systems
- Small systems *(e.g. pp, pPb)*
  - → shorter lifetimes wrt heavy-ion systems
  - → better insight into early system dynamics & initial geometry
- 2-particle BEC analyses for *pp* and *pPb/Pbp* at LHCb
  - → direct comparison of results in two different small systems
  - → additional constraints for theoretical models
  - → what is the origin of correlations in small systems?
- First measurements for *pp* & *pPb* collisions in the forward direction
  - → unique contribution to study dependence of source size on rapidity

Motivation: 3-particle BEC

- Three-particle BEC within core-halo

  → inspired by PHENIX analysis in *Au-Au* [Universe 4 (2018) 57]

  → measure of coherence and thermalization in the source

  → first time in proton-proton collisions in frame of core-halo model

  → helps to answer the question on coherent emission in small systems

- Core-halo model
  [Z. Phys. C71 (1996) 491; EPJ C9 (1999) 275]

  → Core

  - direct production
  - hydrodynamic evolution / particle production from excited strings, followed by subsequent rescattering

  → Halo

  - core surrounded by particles emitted from decay of long-lived hadronic resonances (ω, η, η', K^0)

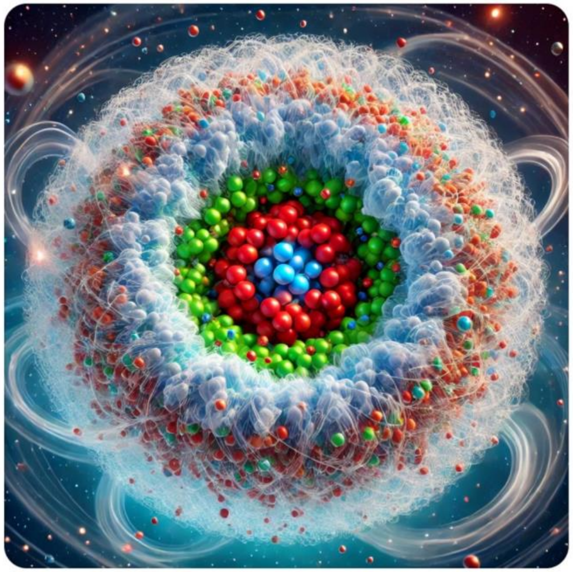

To disentangle partial coherence and halo contribution

→ 2 separate measurements are needed

→ two- and three-particle BEC

LHCb detector

[Int. J. Mod. Phys. A30 (2015) 1530022]

- single arm spectrometer fully instrumented in forward region → GPD in forward region
- designed to study *b/c* hadrons, but also fixed target, heavy ion physics
- precision coverage unique for LHCb: $2 < \eta < 5$
- complementary results wrt other LHC experiments

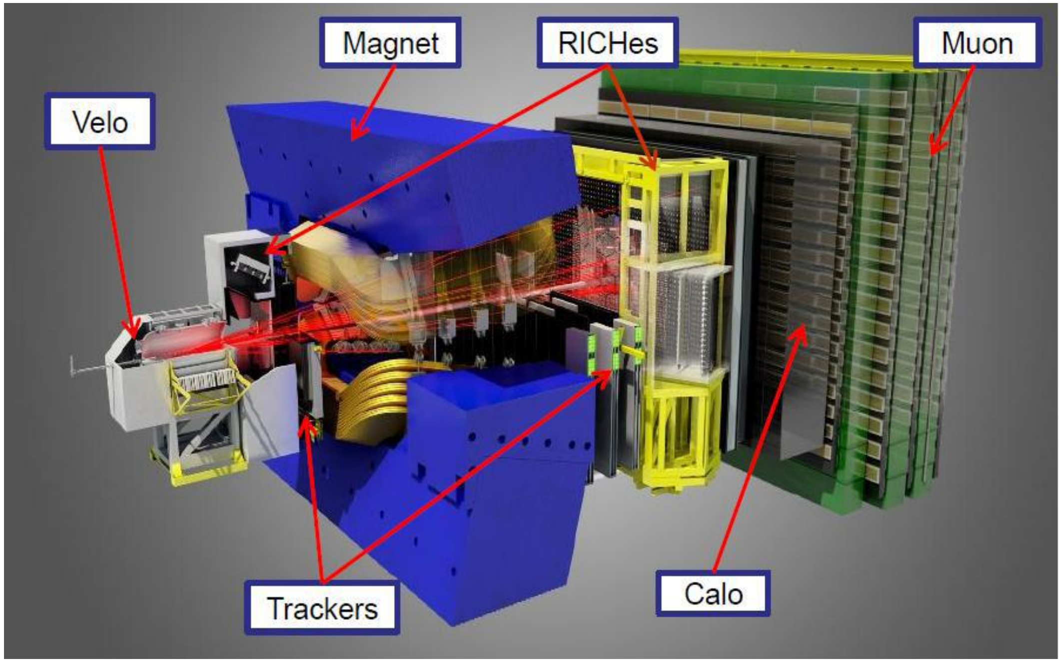

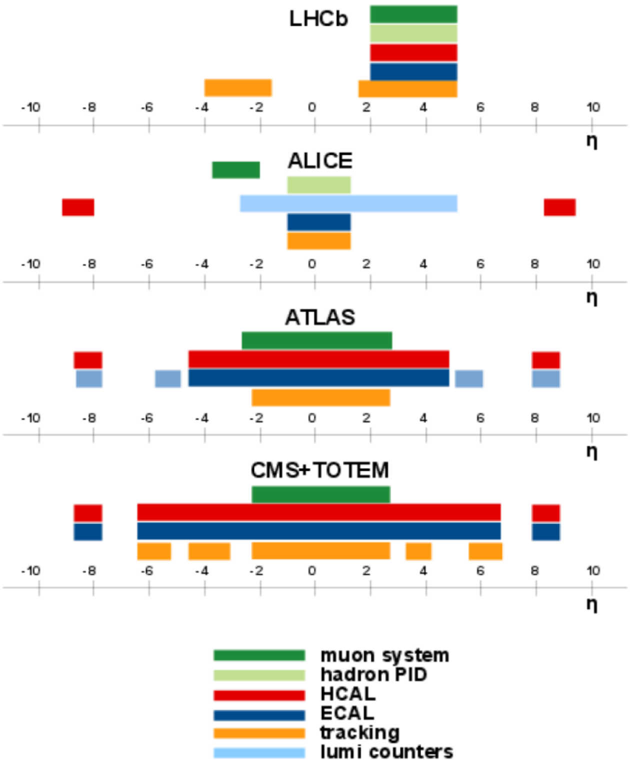

[IJMPA 30 (2015) 1530022]

- momentum resolution between 0.5% at 5 GeV to 1.0% at 200 GeV
- IP resolution of 20 μm for high-p_T tracks
- good PID separation up to 100 GeV *(misID ($\pi \to K$) ≈ 5% at 95% efficiency)*

2-pion BEC at LHCb

[JHEP 12 (2017) 025, JHEP 09 (2023) 172]

Correlation function

[JHEP 12 (2017) 025]

Experimentally: $C_2(Q) = \frac{N(Q)^{DATA}}{N(Q)^{REF}}, \quad REF = mix, MC, unlike$

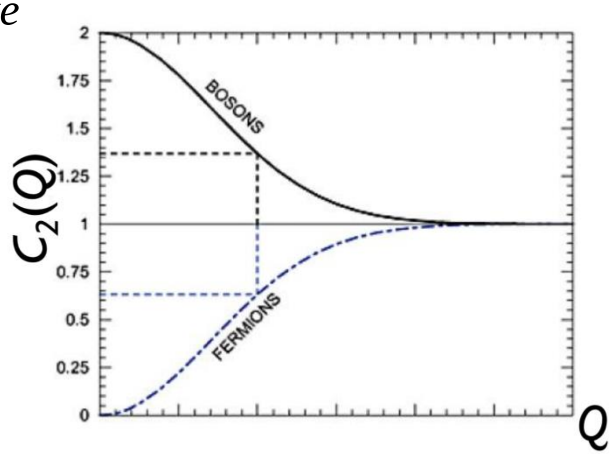

Reference sample

→ event mix: different events, same VELO multiplicity

$$Q = \sqrt{-(q_1 - q_2)^2} = \sqrt{M^2 - 4\mu^2}$$

Parametrization

→ Lévy parametrization with α =1 (Cauchy) + long-range correlations

$$C_2(Q) = N(1 \pm \lambda e^{-|RQ|^\alpha}) \times (1 + \delta \cdot Q)$$

- *R* - radius of spherical static source
- λ - intercept parameter
  (0 – coherent source, 1 – chaotic case)
- *N* - normalisation factor
- δ - long range correlations
- α - Lévy index of stability

Background – BEC in point-like sources ***(pp)***

[JHEP 12 (2017) 025]

DOUBLE RATIO: improved correlation function

$$r_{\mathrm{d}}(Q) \equiv \frac{C_2(Q)^{\mathrm{data}}}{C_2(Q)^{\mathrm{simulation}}}$$

simulation without BEC

- reduce possible imperfections in the construction of the reference sample
- eliminate second order effects to large extent
- correct for long range correlations *(if properly simulated)*

By construction the correlation function is largely independent of

- single particle acceptance and efficiency
- effects due to the detector occupancy, acceptance and material
- selection cuts
- two-track efficiency effects if properly simulated

Background – BEC in extended sources ***(pPb)***

[JHEP 09 (2023) 172]

Parametrization using Bowler-Sinyukov formalism

[Phys. Lett. B270 (1991) 69, Phys. Lett. B432 (1998) 248]

$$C_2(Q) = N\left[1 - \lambda + \lambda K(Q) \times \left(1 + e^{-|RQ|}\right)\right] \times \Omega(Q)$$

Lévy parametrization with index of stability fixed to unity used to describe the BEC effect

[Eur. Phys. J. C36 (2004) 67-78]

Non-femtoscopic background studied using DATA in $C_2(Q)$ for oppositely-charged (OS) pions

→ no theoretical models describing the shape of the non-femtoscopic background

→ ad-hoc parametrizations commonly used to describe the data

- ***cluster contribution:*** *reasonable description in low-Q region using simple Gaussian with* A_{bkg} *and* σ_{bkg}
- ***long-range correlations:*** *commonly used linear form with factor* δ

$$\Omega(Q) = \underbrace{(1 + \delta Q)}_{\text{long-range correlations}} \times \underbrace{\left[1 + z\frac{A_{\text{bkg}}}{\sigma_{\text{bkg}}\sqrt{2\pi}} \exp\left(-\frac{Q^2}{2\sigma_{\text{bkg}}^2}\right)\right]}_{\text{cluster contribution}}$$

[Phys. Rev. C97 (2018) 064912]

Removal of resonances that may disturb the background fit

pPb/Pbp – removal of resonances

[JHEP 09 (2023) 172]

- Goal is to remove most peaking ones that may significantly disturb the background fit
  not aiming to completely remove all the Q-regions affected by resonances

- Effects related to resonances wear off quickly with growing particle multiplicity

- Choice of both list of resonances and widths of excluded ranges optimized in similar analyses *(e.g. Phys. Rev. C96 (2017) 064908, Phys. Rev. C97 (2018) 064912)*

resonance	Q range [GeV]
$\rho^0(770)$	0.55–0.88
$K^0_{\mathrm{S}}(497)$	0.38–0.44
$f_0(980)$	0.91–0.97
$f_2(1270)$	1.21–1.27

- Effects related to resonance removal are included in systematics with relatively small contribution *(max. 4%)*

Coulomb effect

[JHEP 12 (2017) 025]
[JHEP 09 (2023) 172]

Point-like sources (*pp*)

Removed with Gamov penetration factor for Q distribution in data:

$$G_2(Q) = \frac{2\pi\zeta}{e^{2\pi\zeta}-1}, \quad \text{where} \quad \zeta = \pm\frac{\alpha m}{Q}$$

Extended sources *(pPb)*

$\rightarrow$ full correction *K(Q)*

$\rightarrow$ approximation valid for Levy sources with α = 1,
developed by CMS in *pPb* analysis [Phys. Rev. C97 (2018) 42]

$$K(Q) = K_{Gamov}(Q)\left(1 + \frac{\alpha\pi m R_{\text{eff}}}{1.26 + QR_{\text{eff}}}\right)$$

$$\zeta = \alpha m \,/\, Q$$

$$K^{\text{SS}}_{Gamov}(\zeta) = \frac{2\pi\zeta}{e^{2\pi\zeta}-1}\ , \ K^{\text{OS}}_{Gamov}(\zeta) = \frac{2\pi\zeta}{1-e^{-2\pi\zeta}}$$

• pion pairs *(relatively small source size)*

$\rightarrow$ no significant difference between full correction and simple Gamov factor

Systematics due to Coulomb correction found to be minor

Results: **BEC in *pp***

[JHEP 12 (2017) 025]

Fits to r_d with Levy parametrization for 3 activity bins

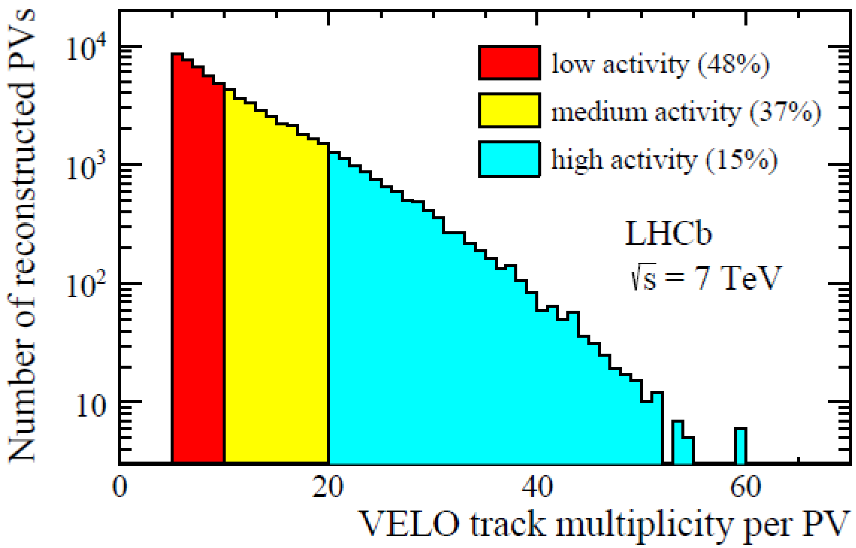

Activity	N_{ch}	R [fm]	λ
Low	[8,18]	$1.01 \pm 0.01 \pm 0.10$	$0.72 \pm 0.01 \pm 0.05$
Medium	[19,35]	$1.48 \pm 0.02 \pm 0.17$	$0.63 \pm 0.01 \pm 0.05$
High	[36,96]	$1.80 \pm 0.03 \pm 0.16$	$0.57 \pm 0.01 \pm 0.03$

Systematic uncertainty (~10%) dominated by the generator tunings and pile-up effects

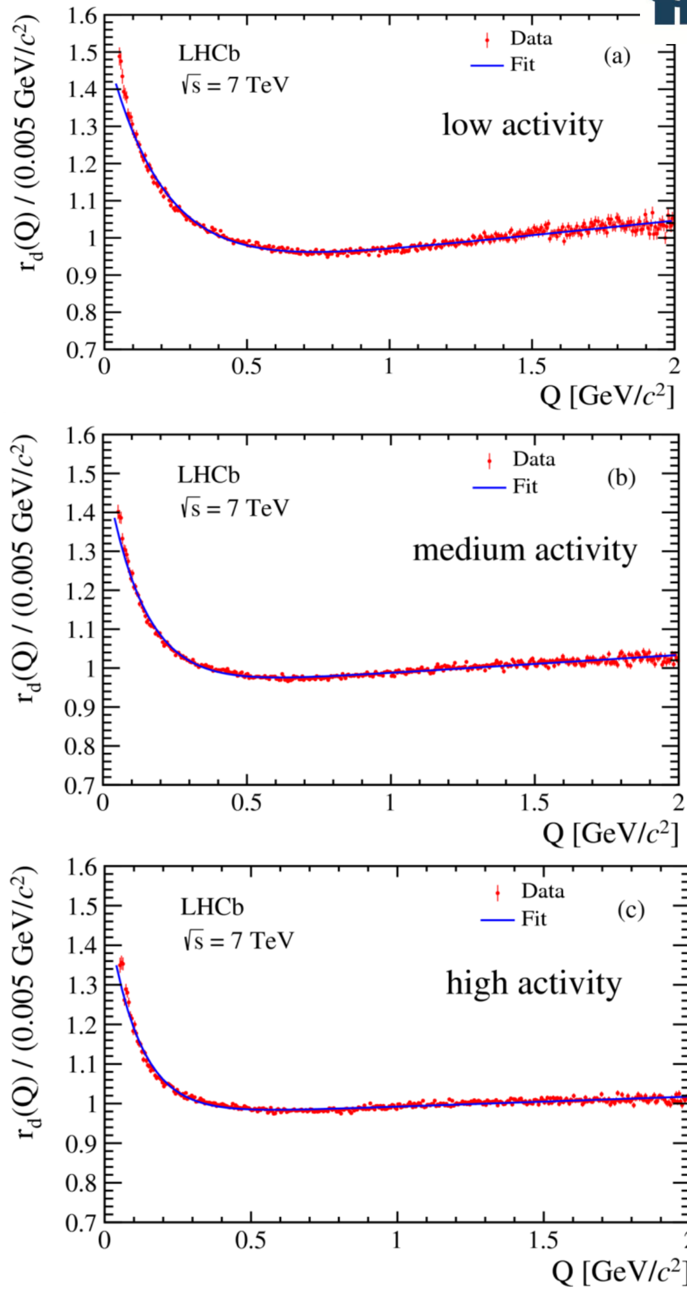

Results: **BEC in *pp***

[JHEP 12 (2017) 025]

Source size increases with activity

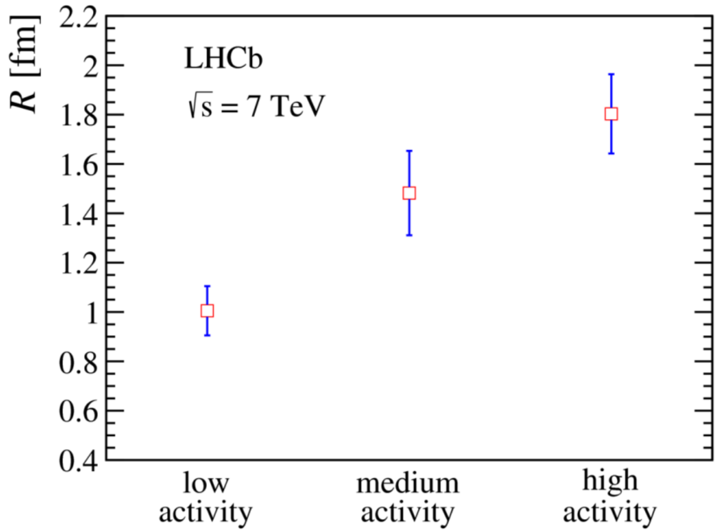

Intercept par. decreases with activity

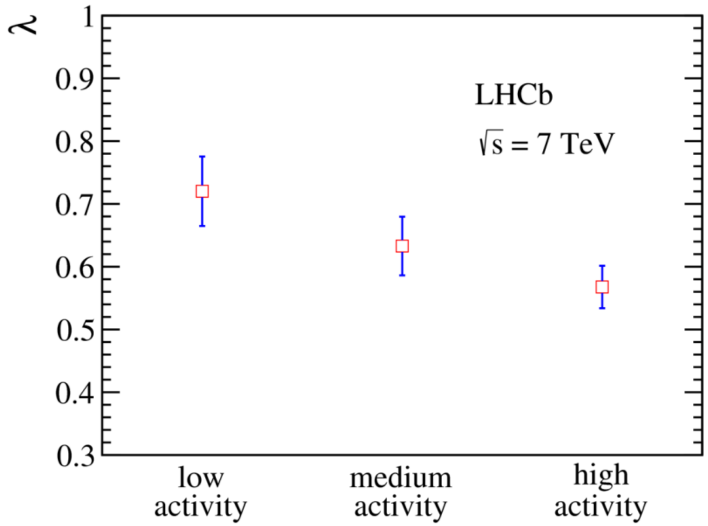

Direct comparison between experiments not straightforward *(different η ranges)*

Trend compatible with previous observations at LEP and other LHC experiments and wrt some theoretical models

R and λ parameters measured in the forward region lower wrt central rapidity detectors, e.g. ATLAS

Setup for proton-lead

- *p-Pb / Pb-p* data collected in 2013 at $\sqrt{s_{NN}}$ = 5 TeV
- **Asymmetric beams:** nucleon-nucleon center-of-mass system shifted by Δy = 0.47 in the proton beam direction

Forward production *(p-Pb)*
rapidity coverage: $1.5 < y_{CMS} < 4.5$
collected data *(2013)*: ~1.1 nb^{-1}

Backward production *(Pb-p)*
rapidity coverage: $-5.5 < y_{CMS} < -2.5$
collected data *(2013)*: ~0.5 nb^{-1}

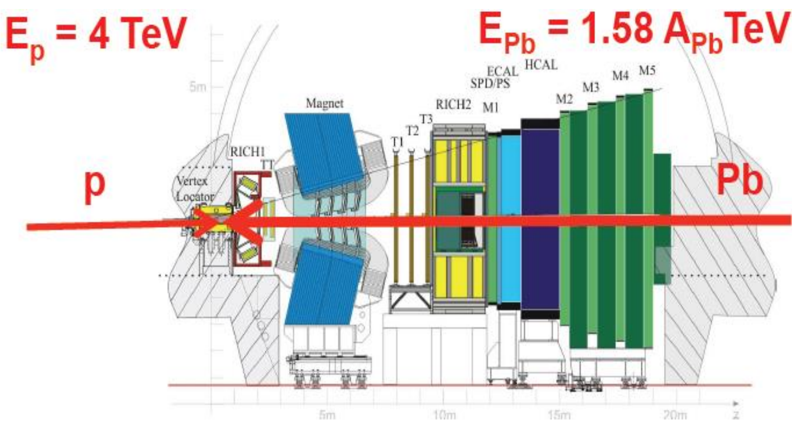

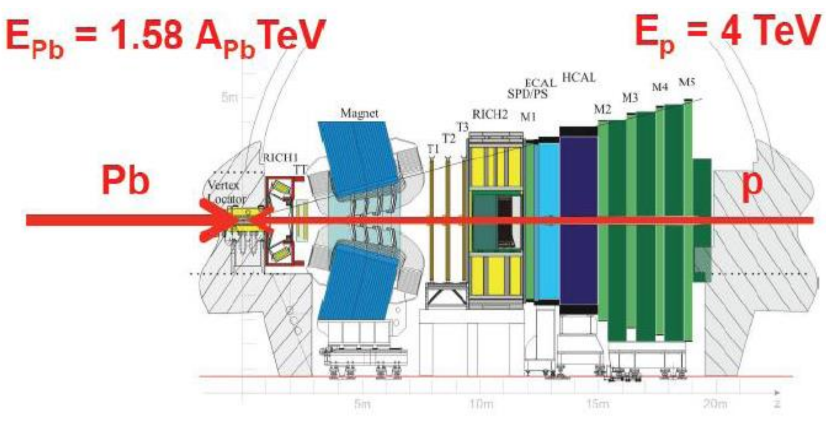

y_{CMS} = rapidity in nucleon-nucleon centre-of-mass system, with forward direction *(positive values)* in direction of the proton/beam

Multiplicity bins *(pPb/Pbp)*

[JHEP 09 (2023) 172]

- Single PV sample
- Common N_{VELO} bins for *pPb/Pbp* to enable direct comparison between *pPb/Pbp* samples

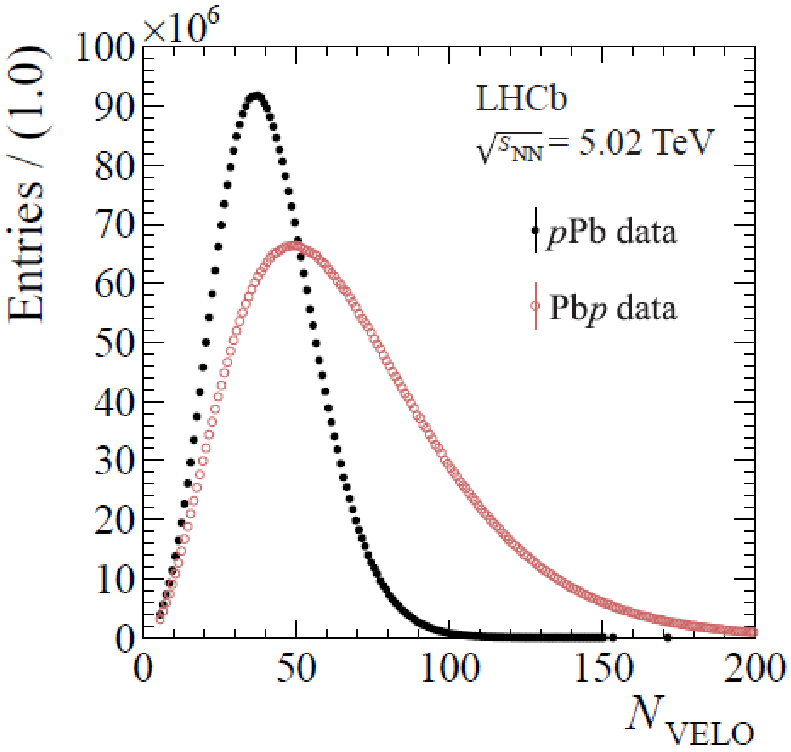

N_{VELO} distribution for signal pairs

N_{VELO} – VELO track multiplicity per PV

		Sample fraction [%]	
bin#	N_{VELO}	pPb	Pbp
1	5–9	< 2	< 2
2	10–14	2	2
3	15–19	4	2
4	20–24	7	3
5	25–29	10	4
6	30–34	13	5
7	35–39	14	6
8	40–44	10	5
9	45–49	10	6
10	50–54	8	6
11	55–59	7	7
12	60–64	5	6
13	65–79	6	15
14	80–89	–	7
15	90–99	–	7
16	100–114	–	6
17	115–139	–	7
18	140–179	–	4

Results: **BEC in *pPb/Pbp***

Fully data-driven approach

Global background fit for opposite sign (OS) pairs

OS fit for *pPb* **OS fit for *Pbp***

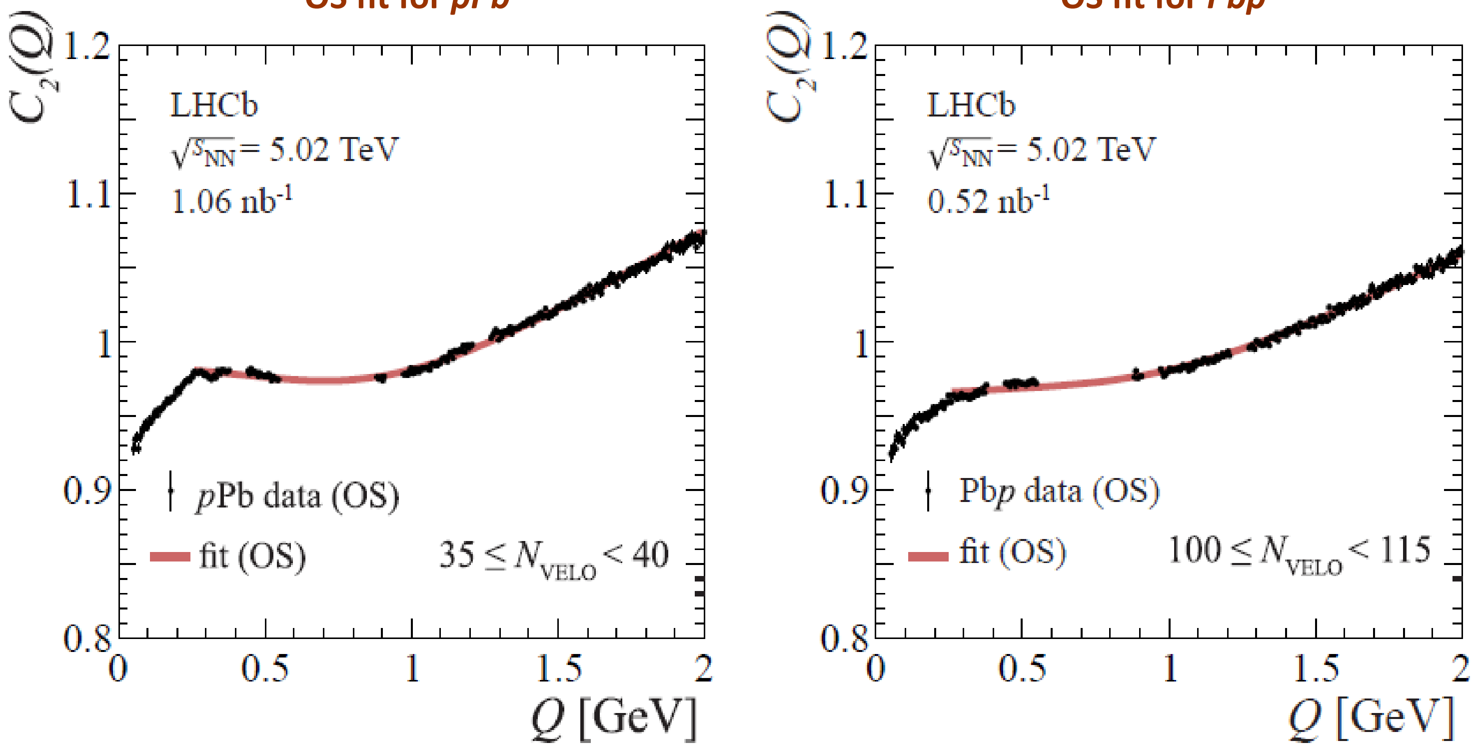

- minFcn/ndf ~2
- 2 separate sets of parameters for *pPb/Pbp* samples
- independent datasets cover different η regions

Results: **BEC in *pPb/Pbp***

[JHEP 09 (2023) 172]

Final fit

- Background parametrization extracted from the OS distributions
- Determine scaling of background amplitude between OS/SS pairs

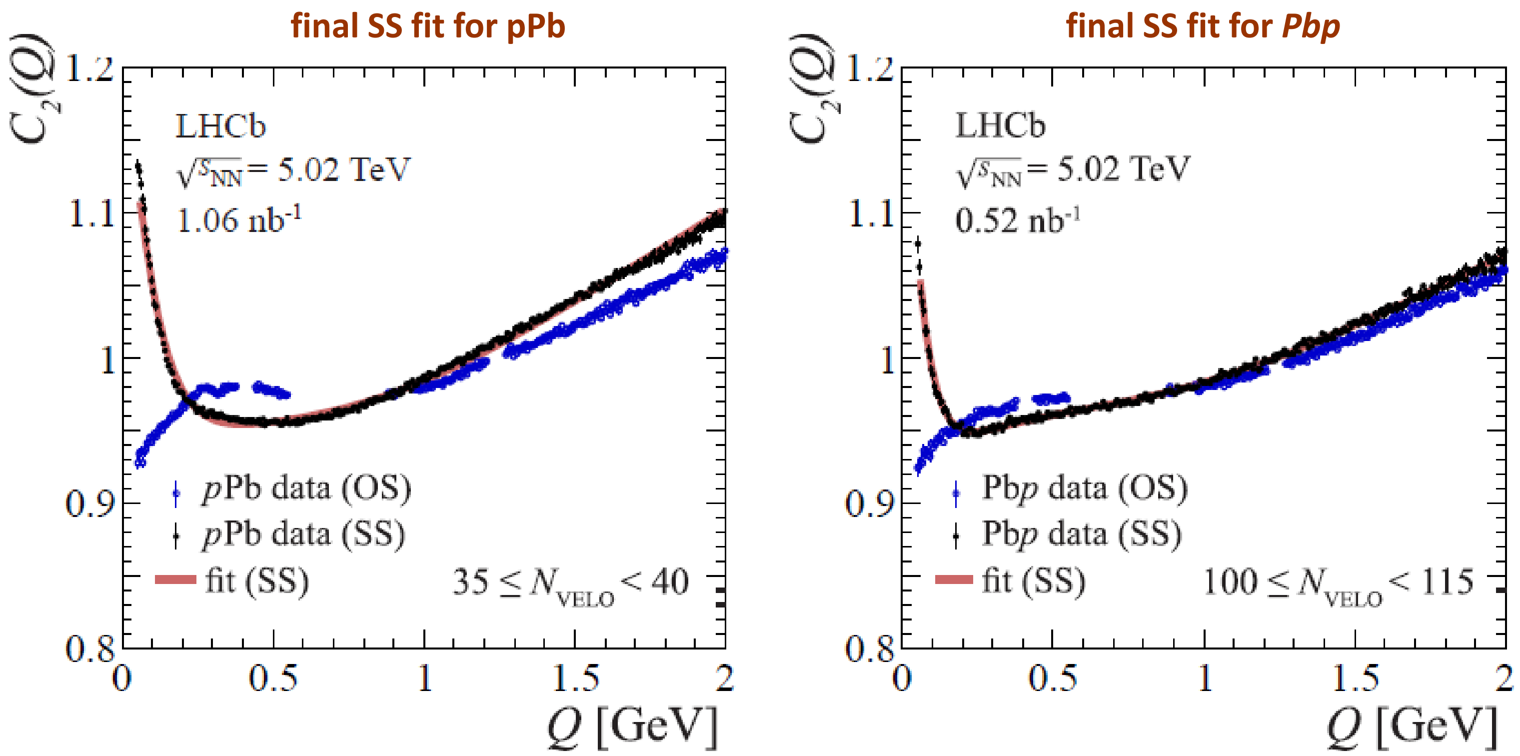

Systematics (from 5% / 6% up to 12.0% / 16.5% for the R / λ parameter)
$\rightarrow$ *dominated by background scaling procedure, pion PID and ghosts removal*

Results: **2-pion BEC**

[JHEP 09 (2023) 172]

- **Scaling of *R* with the cube root of N_{VELO}**

  → *hydrodynamic models?* ***(but α = 1)***

- Two beam modes (*pPb/Pbp*): studying the system in the forward/backward direction

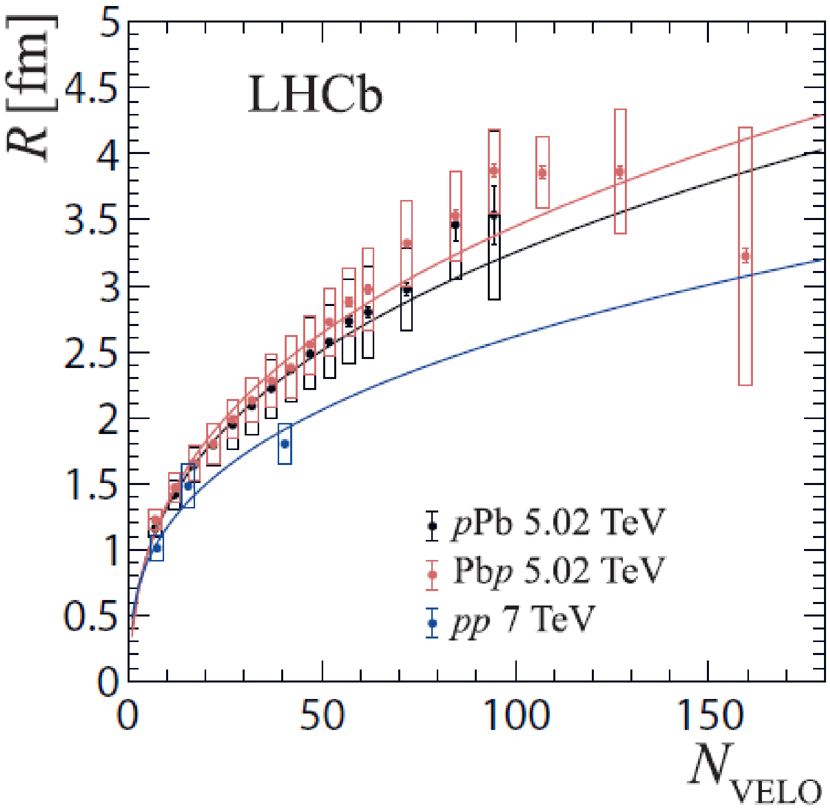

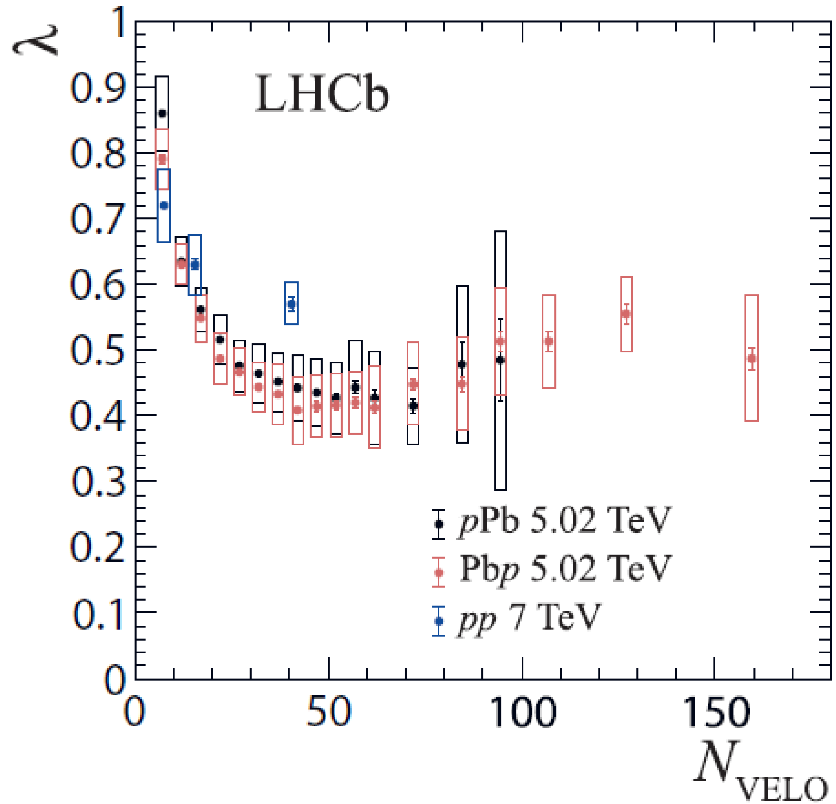

Central *R*-values for *Pbp* sample systematically higher as compared to *pPb*

→ *hints for the dependence of correlation parameters on rapidity*

3-pion BEC at LHCb

[JHEP 08 (2025) 174]

Three-particle BEC within core-halo model

[JHEP 08 (2025) 174]

First time in proton-proton collisions in frame of core-halo model

$$C_3(Q_{12},Q_{13},Q_{23}) =$$
$$N(1+\delta_{12}Q_{12})(1+\delta_{13}Q_{13})(1+\delta_{23}Q_{23})G_3(Q_{12},Q_{13},Q_{23})C_3^{(0)}(Q_{12},Q_{13},Q_{23})$$

- Convolution of 2-particle correlation functions
  [T. Novak, arXiv:1801.03544; Universe 4 (2018) 57]

$$C_3^{(0)}(Q_{12},Q_{13},Q_{23}) = C_2^{(0)}(Q_{12})C_2^{(0)}(Q_{13})C_2^{(0)}(Q_{23})$$

- Coulomb corrections

  → factorized according to Generalized Riverside Method
  [Phys. Rev. C 92, 014902]

$$G_3(Q_{12},Q_{13},Q_{23}) \approx G_2(Q_{12})G_2(Q_{13})G_2(Q_{23})$$

- Lévy-type three-pion correlation function of the Q_{12}, Q_{13}, Q_{23} of the pion triplet
  [T. Novak, arXiv:1801.03544]

$$C_3(Q_{12},Q_{13},Q_{23}) = N(1+\delta_{12}Q_{12})(1+\delta_{13}Q_{13})(1+\delta_{23}Q_{23})G_2(Q_{12})G_2(Q_{13})G_2(Q_{23})$$
$$(1+\ell_3 e^{-0.5|R(Q_{12}+Q_{13}+Q_{23})|} + \ell_2(e^{-|Q_{12}R|} + e^{-|Q_{13}R|} + e^{-|Q_{23}R|})),$$

- $\boxed{\lambda_3 = \ell_3 + 3\ell_2\text{, } R \text{ and } \lambda_2 \text{ taken from 2-pion BEC at LHCb}}$ [JHEP 12 (2017) 025]

Fit to 3-pion double ratio

[JHEP 08 (2025) 174]

- 3 bins of VELO track multiplicity
- assumption of diagonal: $Q_{12} = Q_{13} = Q_{23}$

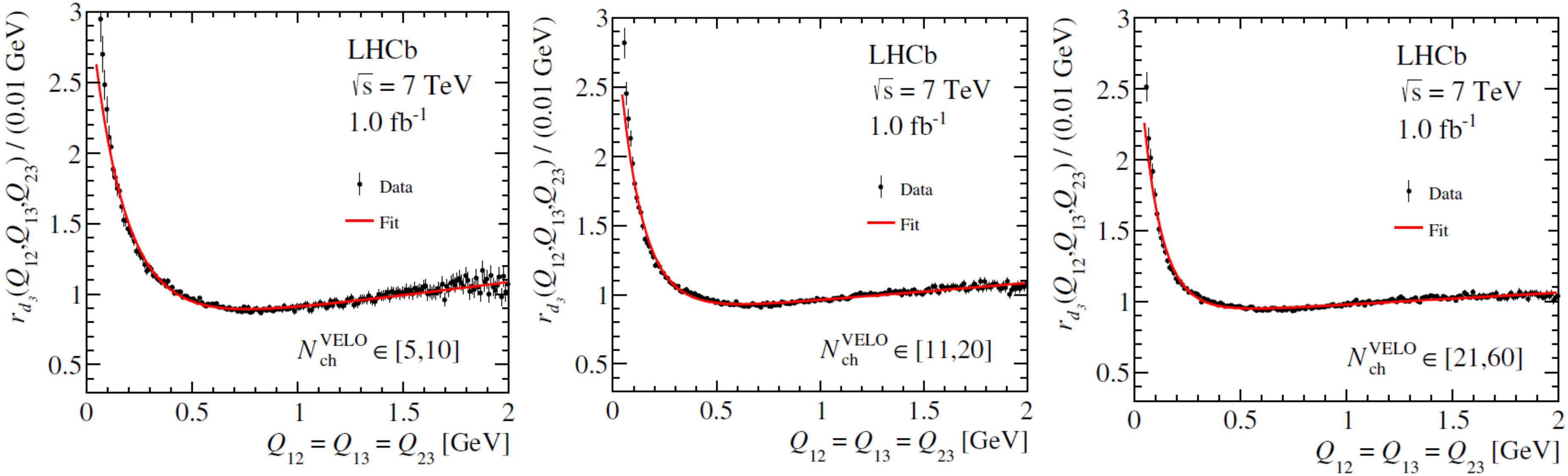

R and λ_2 taken from two-pion analysis

$\rightarrow$ x-checked to be compatible with present analysis

Core-halo model parameters

[JHEP 08 (2025) 174]

Fraction of the core: $f_c = \frac{N_{core}}{N_{core} + N_{halo}}$

Partial coherence: $p_c = \frac{N_{coherent}}{N_{coherent} + N_{incoherent}}$

2- and 3-particle correlation strengths related to f_c and p_c:

$$f_c^2[(1-p_c)^2 + 2p_c(1-p_c)] = \lambda_2$$
$$2f_c^3[(1-p_c)^3 + 3p_c(1-p_c)^2] + 3f_c^2[(1-p_c)^2 + 2p_c(1-p_c)] = \lambda_3$$

Parameter independent of fraction of particles originating from core

$$\kappa_3 = 0.5(\lambda_3 - 3\lambda_2)/\lambda_2^{3/2}$$

[T. Novak, arXiv:1801.03544]

→ *describes additional effects like partial coherence or not fully thermalized core*

→ *potential to challenge the boundaries of the core-halo model*

Results: **3-pion BEC**

[JHEP 08 (2025) 174]

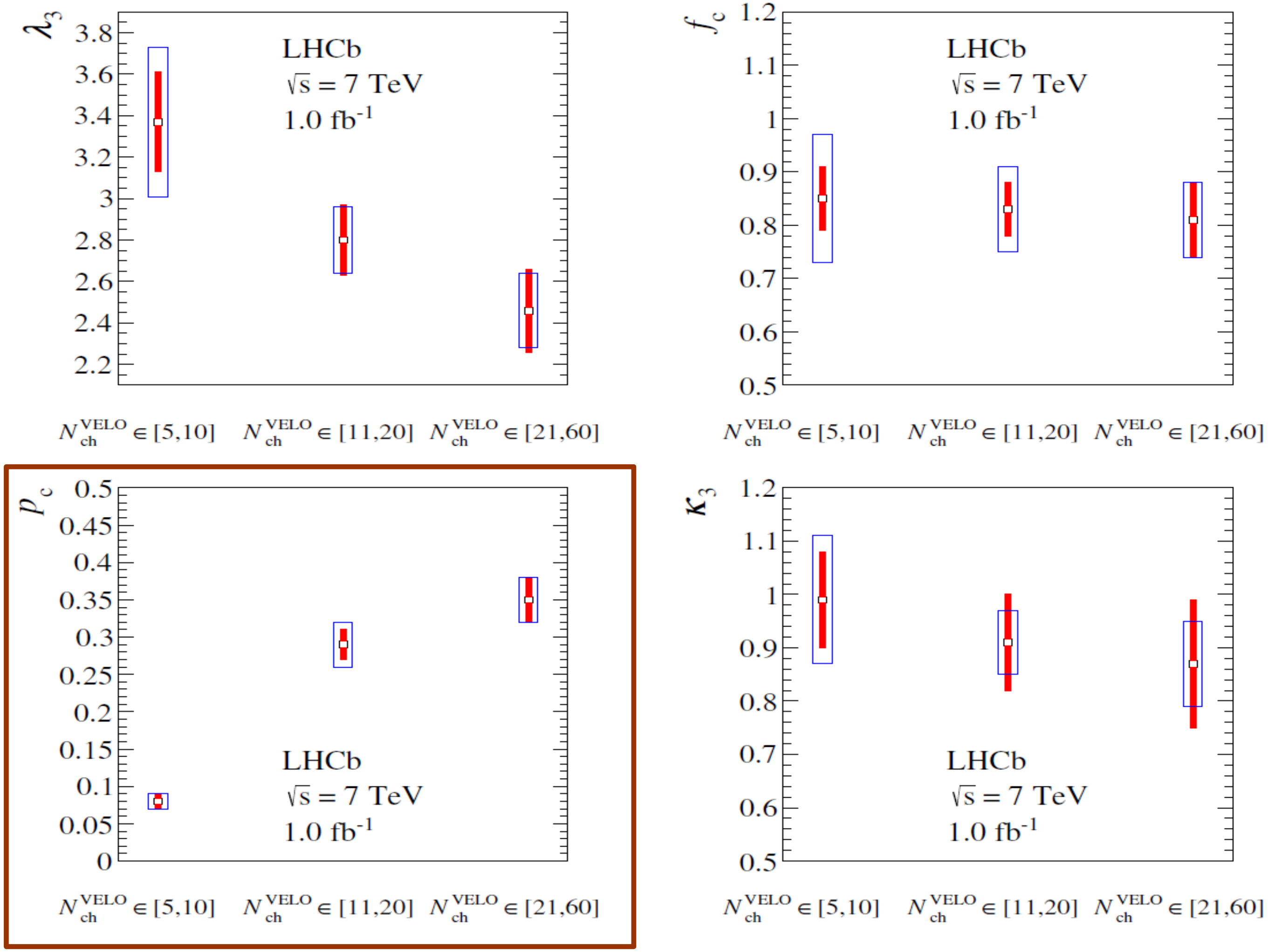

- **partial coherence p_c increases significantly with charged particle multiplicity**
- κ_3 systematically below unity, but still within uncertainties

Results: **3-pion BEC**

[JHEP 08 (2025) 174]

f_c (fraction of core)

$\rightarrow$ decreases only slightly with multiplicity

$\rightarrow$ fraction of particles originating from core not depend strongly on multiplicity

p_c (partial coherence)

$\rightarrow$ increases significantly with higher multiplicity

$\rightarrow$ **shows presence of partially coherent emission of pions**

κ_3 parameter

$\rightarrow$ central values systematically below unity for higher-multiplicities

$\rightarrow$ however consistent with unity within errors

$\rightarrow$ supports partially coherent emission observed in p_c

Conclusions

BEC studied in 2 types of small systems (*pp/pPb*)

Both 2-pion studies → first measurements of BEC in forward region

- 2 alternative methods for non-femtoscopic background
- scaling of R with cube root of N_{ch} **(hydrodynamic models? but α = 1)**
- hints for dependence of correlation parameters on rapidity

3-pion BEC in *pp* within core-halo model

- first time in *pp* with interpretation using core-halo
- **measured parameter (p_c) shows partially coherent emission of pions**
- 2- and 3-particle BEC used to disentangle partial coherence and halo

Backup

HBT interferometry

1950s: R. Hanbury Brown and R. Q. Twiss

- correlations between photons from different points on source surface
- consequence of the Bose-Einstein statistics

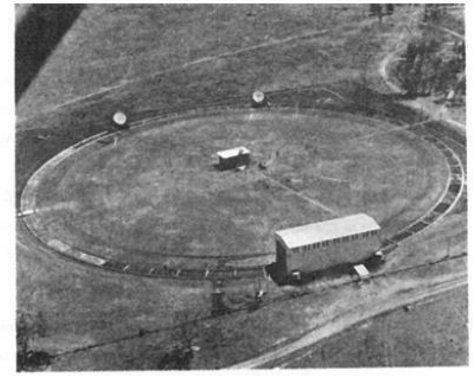

Hanbury Brown-Twiss (HBT) interferometry

- identical particle interferometry usually identified with HBT
- intensity interferometry used to measure the diameters of distant radio sources

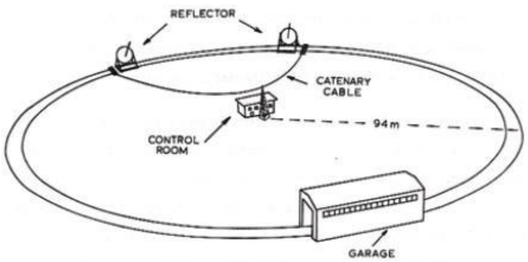

Changing distance between detectors → measure diameter of emitting source

$$C_2(\vec{r}) = \frac{\langle I_1 I_2 \rangle}{\langle I_1 \rangle \langle I_2 \rangle} \sim 1 + \cos\left(\vec{k} \cdot \Delta\vec{r}\right)$$

$\Delta\vec{r}$ – source size

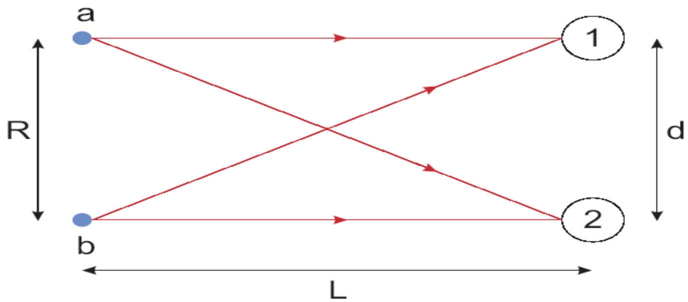

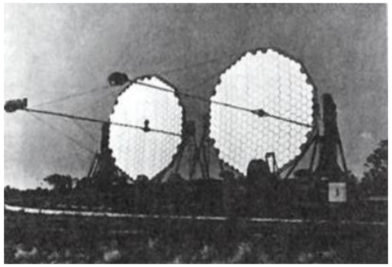

pPb/Pbp – results

[JHEP 09 (2023) 172]

	pPb dataset		Pbp dataset	
N_{VELO}	R [fm]	λ	R [fm]	λ
5–9	$1.159 \pm 0.010 \pm 0.070$	$0.860 \pm 0.006 \pm 0.056$	$1.227 \pm 0.013 \pm 0.080$	$0.791 \pm 0.007 \pm 0.045$
10–14	$1.413 \pm 0.010 \pm 0.105$	$0.635 \pm 0.004 \pm 0.037$	$1.469 \pm 0.013 \pm 0.108$	$0.630 \pm 0.005 \pm 0.031$
15–19	$1.638 \pm 0.011 \pm 0.131$	$0.562 \pm 0.004 \pm 0.033$	$1.658 \pm 0.014 \pm 0.135$	$0.548 \pm 0.005 \pm 0.036$
20–24	$1.790 \pm 0.011 \pm 0.161$	$0.516 \pm 0.004 \pm 0.036$	$1.801 \pm 0.015 \pm 0.148$	$0.487 \pm 0.005 \pm 0.038$
25–29	$1.944 \pm 0.012 \pm 0.189$	$0.476 \pm 0.004 \pm 0.039$	$1.989 \pm 0.017 \pm 0.150$	$0.467 \pm 0.005 \pm 0.036$
30–34	$2.088 \pm 0.014 \pm 0.214$	$0.464 \pm 0.004 \pm 0.044$	$2.130 \pm 0.019 \pm 0.169$	$0.444 \pm 0.005 \pm 0.037$
35–39	$2.218 \pm 0.016 \pm 0.225$	$0.452 \pm 0.005 \pm 0.044$	$2.279 \pm 0.021 \pm 0.206$	$0.433 \pm 0.006 \pm 0.045$
40–44	$2.364 \pm 0.019 \pm 0.250$	$0.443 \pm 0.005 \pm 0.049$	$2.380 \pm 0.024 \pm 0.233$	$0.409 \pm 0.006 \pm 0.051$
45–49	$2.482 \pm 0.023 \pm 0.271$	$0.435 \pm 0.006 \pm 0.052$	$2.554 \pm 0.027 \pm 0.220$	$0.415 \pm 0.007 \pm 0.047$
50–54	$2.575 \pm 0.028 \pm 0.281$	$0.427 \pm 0.008 \pm 0.053$	$2.725 \pm 0.031 \pm 0.259$	$0.416 \pm 0.008 \pm 0.048$
55–59	$2.730 \pm 0.036 \pm 0.322$	$0.443 \pm 0.010 \pm 0.070$	$2.875 \pm 0.035 \pm 0.252$	$0.420 \pm 0.009 \pm 0.046$
60–64	$2.799 \pm 0.046 \pm 0.341$	$0.427 \pm 0.012 \pm 0.070$	$2.972 \pm 0.040 \pm 0.306$	$0.412 \pm 0.010 \pm 0.062$
65–79	$2.972 \pm 0.045 \pm 0.318$	$0.415 \pm 0.011 \pm 0.059$	$3.322 \pm 0.028 \pm 0.324$	$0.448 \pm 0.007 \pm 0.062$
80–89	$3.462 \pm 0.115 \pm 0.410$	$0.479 \pm 0.033 \pm 0.118$	$3.531 \pm 0.043 \pm 0.337$	$0.449 \pm 0.011 \pm 0.070$
90–99	$3.535 \pm 0.219 \pm 0.635$	$0.485 \pm 0.062 \pm 0.196$	$3.871 \pm 0.052 \pm 0.320$	$0.513 \pm 0.015 \pm 0.081$
100–114	–	–	$3.854 \pm 0.049 \pm 0.270$	$0.513 \pm 0.015 \pm 0.072$
115–139	–	–	$3.863 \pm 0.049 \pm 0.468$	$0.555 \pm 0.016 \pm 0.057$
140–179	–	–	$3.225 \pm 0.053 \pm 0.979$	$0.487 \pm 0.016 \pm 0.096$

pPb/Pbp – systematics

[JHEP 09 (2023) 172]

Listed ranges correspond to the lowest and highest values of the given input determined across most of the N_{VELO} bins in the *pPb* and *Pbp* samples

	pPb dataset		Pbp dataset	
Contribution	$\sigma_{\text{syst}}(R)$ [%]	$\sigma_{\text{syst}}(\lambda)$ [%]	$\sigma_{\text{syst}}(R)$ [%]	$\sigma_{\text{syst}}(\lambda)$ [%]
Background scaling	4.5–9.0	3.5–11.0	4.5–6.5	3.0–9.5
Background fit range	1.0–3.0	0.5–3.5	2.0–3.5	0.5–4.0
Background fit – fixed N_0	0.5–3.0	0.5–3.0	< 0.5	< 0.5
Background fit – resonances	0.5–4.0	0.5–4.0	1.5–3.0	0.5–3.5
PID optimisation	0.5–1.5	0.5–5.0	0.5–10.5	0.5–8.5
Fake tracks	0.5–5.5	1.0–8.0	0.5–4.5	0.5–8.0
Requirement on z_{PV}	0.5–1.5	0.5–3.0	0.5–2.0	0.5–3.5
Coulomb correction	0.5–1.5	1.0–2.5	0.5–2.0	0.5–3.0
SS fit range (min)	1.5–5.0	1.0–8.5	0.5–3.5	0.5–5.5
SS fit range (max)	0.5–1.0	0.5–2.0	0.5–2.0	0.5–3.0
Reference sample	0.5–2.0	0.5–3.0	0.5–2.0	0.5–4.0
Total	6.0–12.0	6.0–16.5	6.5–12.0	5.0–16.0

Negligible contributions not listed

pPb/Pbp – global background fit

[JHEP 09 (2023) 172]

Correlation function for opposite sign pairs

$$C_2^{\mathrm{OS}}(Q) = N \times K(Q) \times \Omega(Q)$$

- Background parameters determined in global OS fit in all N_{VELO} bins
- Negative log-likelihood function minimized for all bins simultaneously
- Common background parameters across bins and free *N*, *δ*

$$\sigma_{\mathrm{bkg}}\left(N_{\mathrm{VELO}}\right) = \sigma_0 + \sigma_1 \exp\left(-\frac{N_{\mathrm{VELO}}}{N_0}\right) \qquad A_{\mathrm{bkg}}\left(N_{\mathrm{VELO}}\right) = \frac{A_0}{\left(N_{\mathrm{VELO}}\right)^{n_A}}$$

[Phys. Rev. C97 (2018) 064912]

- best stability of fits obtained with fixed scale N_0 of multiplicity dependence for σ_{bkg}
- the value based on the results obtained with N_0 free for the *pPb* sample
- choice of this scale is studied in systematics

pPb/Pbp – removal of resonances

[JHEP 09 (2023) 172]

- Goal is to remove most peaking ones that may significantly disturb the background fit
  not aiming to completely remove all the Q-regions affected by resonances

- Effects related to resonances wear off quickly with growing particle multiplicity

- Choice of both list of resonances and widths of excluded ranges optimized in similar analyses *(e.g. Phys. Rev. C96 (2017) 064908, Phys. Rev. C97 (2018) 064912)*

resonance	Q range [GeV]
$\rho^0(770)$	0.55–0.88
$K^0_S(497)$	0.38–0.44
$f_0(980)$	0.91–0.97
$f_2(1270)$	1.21–1.27

- Effects related to resonance removal are included in systematics with relatively small contribution *(max. 4%)*

pPb/Pbp – background scaling

[JHEP 09 (2023) 172]

As the cluster contribution is expected to be larger for OS pairs as compared to SS ones, due to charge conservation, additional scaling factor is introduced with a theoretically motivated form (OS/SS pairs combinatorics):

$$z(N_{\mathrm{VELO}}) = \frac{aN_{\mathrm{VELO}} + b}{1 + aN_{\mathrm{VELO}} + b}$$

Parameters *a* and *b* are determined by first fitting same-sign pair correlation function in each bin with fixed background and *z* as free parameter, and then performing fit of $z(N_{VELO})$

In low multiplicity bins the distortions related to background / resonances etc. are more prominent

- expect to have more significant fluctuations in the fits in such bins

This is why we follow theoretically-motivated method *(used also e.g. in Phys. Rev. C97 (2018) 064912 or JHEP 03 (2020) 014)* **to have a smooth description in all multiplicity bins**

- avoid in this way transmitting such fluctuations to the final SS fits
- avoid potential biases in the final results

Exact shape of the *z* distribution not so relevant

- we study the systematic uncertainty related to this method

3-pion BEC - selection

[JHEP 08 (2025) 174]

Main goal:

- unbiased, high-purity sample of prompt pions
- good track quality and PV assignment
- reduction of clones / ghosts

selection	requirement
track type	long, charged, no muon signature no shared VELO segments
track η	2.0–5.0
track χ^2	< 2.0
track p	$> 2.0\,\mathrm{GeV}$
track p_{T}	$> 0.1\,\mathrm{GeV}$
track IP	$< 0.4\,\mathrm{mm}$
$ProbNN$(ghost)	< 0.25
$ProbNN$(kaon,proton)	< 0.50
$ProbNN$(pion)	> 0.65
pair $\lvert\Delta t_x\rvert, \lvert\Delta t_y\rvert$	$\lvert\Delta t_x\rvert > 0.3\times10^{-3}$ OR $\lvert\Delta t_y\rvert > 0.3\times10^{-3}$
pair Q	$> 0.05\,\mathrm{GeV}$

$\Delta t_x, \Delta t_y$: differences in the track slopes in a pair in the *x* and *y* directions

3-pion BEC – results

[JHEP 08 (2025) 174]

parameters of the fit to three-pion double ratio

	$N_{\rm ch}^{\rm VELO} \in [5,10]$	$N_{\rm ch}^{\rm VELO} \in [11,20]$	$N_{\rm ch}^{\rm VELO} \in [21,60]$
χ^2/ndf	170/191	285/191	262/191
N	0.74 ± 0.01	0.85 ± 0.01	0.90 ± 0.01
ℓ_2	0.47 ± 0.05	0.52 ± 0.03	0.46 ± 0.05
ℓ_3	1.93 ± 0.19	1.25 ± 0.15	1.08 ± 0.18
δ	0.07 ± 0.01	0.04 ± 0.01	0.03 ± 0.01

$N_{\rm ch}^{\rm VELO} \in [5,10]$
$\lambda_3 = 3.37 \pm 0.24 \pm 0.37$
$f_c = 0.85 \pm 0.06 \pm 0.12$
$p_c = 0.08 \pm 0.01 \pm 0.01$
$\kappa_3 = 0.99 \pm 0.09 \pm 0.12$

$N_{\rm ch}^{\rm VELO} \in [11,20]$
$\lambda_3 = 2.80 \pm 0.17 \pm 0.16$
$f_c = 0.83 \pm 0.05 \pm 0.07$
$p_c = 0.29 \pm 0.02 \pm 0.03$
$\kappa_3 = 0.91 \pm 0.09 \pm 0.06$

$N_{\rm ch}^{\rm VELO} \in [21,60]$
$\lambda_3 = 2.46 \pm 0.20 \pm 0.18$
$f_c = 0.81 \pm 0.07 \pm 0.07$
$p_c = 0.35 \pm 0.03 \pm 0.03$
$\kappa_3 = 0.87 \pm 0.12 \pm 0.08$

3-pion BEC – systematics

[JHEP 08 (2025) 174]

$N_{\rm ch}^{\rm VELO} \in [5,10]$

Source	σ_{λ_3} [%]	σ_{f_c} [%]	σ_{p_c} [%]	σ_{κ_3} [%]
Event generator	8.7	10.4	9.7	10.4
PV multiplicity	5.9	8.6	8.3	4.7
PV reconstruction	< 0.1	0.1	0.1	< 0.1
Fit binning	0.7	0.1	0.4	1.2
Fit low-Q range	0.3	0.6	1.0	0.3
Fit high-Q range	0.4	0.5	0.5	0.3
Fake tracks	2.1	2.4	2.4	1.8
$\mathcal{P}(\pi)$	2.1	2.7	1.8	3.3
Total	11.0	14.0	13.2	12.1

$N_{\rm ch}^{\rm VELO} \in [11,20]$

Source	σ_{λ_3} [%]	σ_{f_c} [%]	σ_{p_c} [%]	σ_{κ_3} [%]
Event generator	3.6	5.1	5.0	3.2
PV multiplicity	2.1	5.0	5.0	2.1
PV reconstruction	1.1	1.6	1.6	1.1
Fit binning	1.1	1.1	1.1	1.1
Fit low-Q range	1.4	1.5	1.8	2.5
Fit high-Q range	1.8	1.9	1.8	2.1
Fake tracks	1.8	4.3	4.3	1.8
$\mathcal{P}(\pi)$	2.1	1.7	1.4	3.9
Total	5.7	9.0	9.0	6.8

$N_{\rm ch}^{\rm VELO} \in [21,60]$

Source	σ_{λ_3} [%]	σ_{f_c} [%]	σ_{p_c} [%]	σ_{κ_3} [%]
Event generator	2.4	2.8	2.8	0.4
PV multiplicity	3.3	5.3	5.4	3.7
PV reconstruction	2.4	2.5	2.4	2.8
Fit binning	1.0	0.4	0.7	2.0
Fit low-Q range	1.8	2.4	3.0	3.7
Fit high-Q range	3.0	3.4	3.4	3.3
Fake tracks	2.0	2.1	2.2	2.4
$\mathcal{P}(\pi)$	4.1	3.9	3.7	5.7
Total	7.5	8.9	9.1	9.4

Negligible contributions not listed